



Low CO<sub>2</sub> footprint on Press Hardened Steels

## Deliverable 1.1

### Comprehensive overview of the project

<b>Project ref. no.</b>	101112485
<b>Project title</b>	Low CO <sub>2</sub> footprint on Press Hardened Steels
<b>Project duration</b>	1 <sup>st</sup> July 2023 – 31 <sup>st</sup> December 2026 (42 months)
<b>Related WP/Task</b>	WP1
<b>Dissemination level</b>	PU-PUBLIC
<b>Deliverable type</b>	REPORT
<b>Document due date</b>	M6 (Dec 2023)
<b>Actual delivery date</b>	M7 (Jan 2023)
<b>Deliverable leader</b>	Eurecat
<b>Document status</b>	Submitted



This project has received funding from the European Union's Research Fund for Coal and Steel (RFCS): project num. 101112485. This document reflects only COOPHS consortium view and neither the European Commission or any associated parties are responsible for any use that may be made of the information it contains.



## Deliverable Information sheet

---

Version	Date	Author	Document history/approvals
0.1	15/12/2023	Jaume Pujante (EUT)	Draft version created
0.2	15/01/2024	Various	Reviewed by all project partners
1.0	31/1/2024	Jaume Pujante (EUT)	Final version produced and submitted



## Executive Summary

---

*The present document provides a comprehensive overview of project COOPHS.*

*This description includes a detailed review of the state of the art related to recycling of high performance steel grades, and how it can affect boron steel grades and press hardened products. It also includes a description of the current knowledge on detailed characterization of segregations and precipitation of tramp elements, using specific techniques based on TEM (Transmission Electron Microscopy) or APT (Atom Probe Tomography). Finally, aspects related to the evaluation of fracture toughness are discussed, together with the implications of Hydrogen Embrittlement.*

*The review of the state of the art is used to formulate the main challenges and gaps in knowledge found in the literature, and discuss how the project is expected to address these gaps and bring additional value.*



## Table of Contents

---

Deliverable Information sheet.....	2
Executive Summary .....	3
Table of Contents .....	4
List of figures .....	5
Terminology and Acronyms.....	5
1. Introduction.....	6
2. State of the Art .....	6
2.1 A Steelmaking Based on EAF Route and Scrap as a Raw Material.....	6
2.2 Residual Elements in Steel.....	6
2.3 Tramp Element Segregation.....	8
2.3.1 Grain Boundary (GB) Segregation .....	8
2.3.2 Surface Segregation .....	11
2.4 Metallurgical Transformations Under the Effect of Tramp Elements .....	13
2.5 Effect of Tramp elements on Ductility and Fracture Behaviour .....	14
2.6 Effect of Tramp Elements on Formability.....	15
2.7 Hydrogen Embrittlement on Tramp Element-Containing Steels .....	16
2.8 Interaction of Tramp Elements with the Coating.....	17
3. Problems Encountered and Proposed Approach.....	18
3.1 Definition of the Problem .....	18
3.1.1 European Steel Industry towards Carbon Neutrality by 2050 .....	18
3.1.2 Materials Production: a new challenge in the race to the Zero Footprint Car .....	19
3.1.3 Press Hardening Steels providing safety and lightweight potential have become key automotive materials .....	19
3.1.4 Low CO <sub>2</sub> Press Hardened Steel production introduces high content of residual elements.....	20
3.1.5 The Impact of residual elements on press hardening steel product requirements is uncertain and could limit the potential of CO <sub>2</sub> emission reductions if not mastered....	21
3.2 COOPHS Approach.....	22
3.2.1 Phase 1: Steelmaking including Residual Elements.....	22
3.2.2 Phase 2: Advanced characterization.....	23
3.2.3 Phase 3: Implications of Tramp Element Segregation on Metallurgy and Performance.....	24
3.2.4 Phase 4: Determination of key relationships between surface and grain boundary segregation of residual element and phase transformation, ductility, toughness and embrittlement behaviors.....	27
3.2.5 Phase 5: Identification of the optimum compromise of CO <sub>2</sub> emission levels and product and application performance of ultrahigh strength press hardened steels.....	27
4. Objectives and Outcomes .....	28
5. References .....	29

## List of figures

---

<i>Figure 1: forecast of “irrecyclable” scrap (with high levels of residuals, including Cu and Sn), proposed in 1997 by (Noro 2017).....</i>	7
Figure 2: Character of individual solutes with respect to the strengthening and embrittling of grain boundaries in bcc iron. Elements marked by green shadows strengthen the grain boundaries in iron, elements marked by red, brown and yellow shadows embrittle them and those marked in grey are indifferent. Red: $\Delta E_{SE,I} > 200$ kJ/mol, brown: $200 > \Delta E_{SE,I} > 90$ kJ/mol, yellow: $90 > \Delta E_{SE,I} > 10$ kJ/mol, grey: $\Delta E_{SE,I} \leq 0$ , dark green: $10 > \Delta E_{SE,I} > 100$ kJ/mol, bright green: $\Delta E_{SE,I} < 100$ kJ/mol, stripped brown/yellow: As, Se, Te and Bi are evident embrittlers but the values of $\Delta E_{SE,I}$ were not presented till now. The effect of the solutes in white fields is unknown. [Kulkov 2018].....	10
Figure 3: Embrittlement potency of P, Cu, Ni and Mn in bcc Fe [He 2017].....	10
Figure 4: APT characterization of a GB of a hot rolled weathering steel containing 0.24%Cu [Guo 2019].....	11
Figure 5: Kinetics of phosphorus surface and grain boundary segregation in a martensitic steel [Cristien 2011].....	12
Figure 6: AES measurements on the surface segregation of Cu, Sn and Sb as a function of soaking temperatures for non-oriented electrical steels [Petrovic 2006].....	12
Figure 7: APT measurement of the surface segregation taking place in the earlier stage of the process (hot rolling) in a low carbon steel with a significant amount of residual elements [Zhang 2022]. .....	13
Figure 8: 3D Atom maps of the as-quenched martensite and chemical composition of the studied grade [Lin 2015].....	14
Figure 9: left: relation between atom size of residual elements and embrittlement (transition temperature shift) [Rod 2006]. right: room temperature Charpy impact energy vs tempering temperature for 4340 steel [Guttman 2001]. .....	15
Figure 10: Loss of hot ductility emphasized by the presence of Cu and Sn in the range 600-800°C for low carbon steels [Peng 2015- Matsuoka 1997]. .....	16
Figure 11: Al, Si and Cu distribution in hot dip and hot stamping coatings with the heating temperature of 850°C [Ziliu 2021]. .....	18
Figure 12: NTS vs CH experimental data, solid line shows the regression curve and shaded areas the confidence interval. Critical hydrogen content (CHcr) is determined in correspondence to a reduction of 30% of tensile strength .....	26

## Terminology and Acronyms

---

BF	Blast Furnace
BOF	Basic Oxygen Furnace
CO2	Carbon Dioxide
EAF	Electric Arc Furnace
EC	European Commission
EU	European Union
GB	Gran Boundary
WP	Work Package



## 1. Introduction

---

The aim of this document is to present a comprehensive overview of the project COOPHS: Low CO<sub>2</sub> Footprint on Press Hardened Steels.

This overview includes an updated and extended description of the state of the art, that helps identifying the challenges of the project and the salient aspects of innovation and impact of the proposed work. The state of the art thus compiled includes aspects of steel recycling in Europe presently and in the future; the effect of residual elements on the metallurgy and properties of the studied steel and, finally, a brief revision of the analysis techniques proposed in the project.

The document also includes a short discussion about the main challenges found and proposed approach, updated reflecting the one year passed between the application and the project start and first meetings.

Finally, a conclusions section is used to re-state the project objectives, and how they relate to the previous discussion.

## 2. State of the Art

---

### 2.1 A Steelmaking Based on EAF Route and Scrap as a Raw Material

Low CO<sub>2</sub> routes for steelmaking are directly associated to the Electric Arc Furnace (EAF) technology for primary metallurgy. Electric arc furnace steelmaking results in lower carbon dioxide emissions of around 600 kg CO<sub>2</sub> per ton of steel produced, which is significantly lower than the conventional production route via blast furnaces - basic oxygen furnace (BOF) estimated beyond 2000 kg CO<sub>2</sub> per ton.

The use of EAFs allows steel to be made from a 100% scrap metal feedstock. If direct-reduced iron (DRI) is available economically, it can also be used as furnace feed and is also the case for hot metal, pig iron and hot briquetted iron [Gyllenram 2015].

### 2.2 Residual Elements in Steel

Residual elements are unwanted alloys that occur in scrap. They may have many different origins: Copper is used in bearings and electrical wire and is often found in recycled steel. Other examples of residual elements are Nickel and Chromium coming from ferritic alloyed steel scrap; and tin and lead which often come from different kinds of coatings and bearings. Scraps are classified according to the content of these residual elements notably Cu and the most widely used in EAF are the categories E1 corresponding to 'Old and Demolition Scrap' with 0.3%Cu, E40 corresponding to 'Shredded Scrap' with 0.2% Cu and E2 and E8 corresponding to 'New Scrap' with low residuals from uncoated metal. (Cu content below 0.04%) [BDSV 1995].

Not all residual elements are equally problematic. It is a well-known fact that some of these residuals oxidize readily into the slag, while others vaporize during EAF melting [Nakajima 2011]. However, some metals typically remain in solution, notably including Cu, Sn, Ni and Mo. Out of these, Copper is of particular importance due to its detrimental effect on hot ductility [Savov 2003] as well as overall abundance in post-consumer scrap [Daehn 2017].

The maximum level of residual elements in steels are set depending on the purpose of the metal products. The EAF scrap feedstock is therefore a tailored mixture of these different scraps. The Cu limit for sheet steels for deep drawing is 0.06% and for standard commercial qualities of hot and cold rolled steel is 0.10% only achievable with high shares of 'New Scrap'.

It is believed that increasing EAF steel volumes will induce a shortage of ‘New Scrap’ and increased share of E40 and E1 and therefore higher Cu and residual elements contents in EAF steels than current ones. This was already posited in the 90s by researchers such as Noro (Noro 1998), pointing to the generation of a category of “irrecyclable” scrap while higher quality material becomes scarcer. This depletion of “high quality” scrap has indeed been observed and described in the EU [Daehn 2017]. Moreover, the gap with BOF routes could be enlarged as typical Cu levels for this route do not exceed 0.03%. This points to a need to reevaluate the Cu thresholds accepted in may steel products.

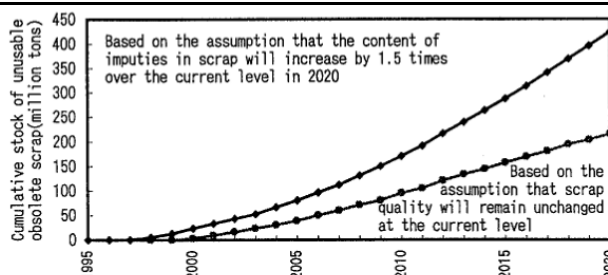


Fig. 7. Results of prediction of the future volume of unrecyclable scrap.

Figure 1: forecast of “irrecyclable” scrap (with high levels of residuals, including Cu and Sn), proposed in 1997 by (Noro 2017)

The EAF process is also prone to produce nitrogen levels higher than BOF productions. EAF is not perfectly sealed, and introduction of nitrogen gas occurs. Nitrogen is ionized during arc formation and rapidly dissolves into the liquid steel leading to values at tapping between 70 and 100ppm. Depending on the secondary metallurgy technology associated downstream (Ladle furnace, Vacuum degassing, etc) the final N content in the product could vary between 80 and 130ppm. This introduces a significant difference with BOF productions where typical N levels at tapping do not exceed 30ppm and can increase up to 50ppm by N pick up during secondary metallurgy without a vacuum degasser [Lee 2015].

The effect of nitrogen on steel properties can be either detrimental or beneficial, depending on the other alloying elements present, the form and quantity of nitrogen present, and the required behavior of the particular steel product. In general, however, most steel products require that nitrogen be kept to a minimum. In B steels Nitrogen plays a particular role as boron must remain in its “free” form i.e., in solid solution in austenite. Boron has high affinity nitrogen to combine readily to form BN during steel making with no possibility of decomposing and dissolving in austenite downstream. Thus, during steel making, boron is protected by addition of a strong nitride former Ti prior to the addition of boron. The drawback of this practice is the formation in the liquid steel of coarse TiN particles with particle diameters from 0.5 to more than 5µm in diameter. The mass fraction of TiN precipitates increases with the product of titanium and nitrogen contents.

The nitrogen level associated to EAF process can be reduced by increasing the share of DRI in the feedstock. The DRI produced by natural gas-based shaft furnaces contains between 2 and 2.5%C. During melting, the DRI produces an effect of ‘washing up’ the excessive nitrogen by the production of CO. To reach a level of nitrogen typical of BOF routes the share of DRI would need to exceed 70% with unfavorable consequences in terms of costs and CO2 emissions [Brosse 2022]. DRI from H2 based reduction processes cannot bring this beneficial effect as its composition is free of carbon.

Phosphorus is a typical minor constituent which is in many steels regarded as impurity and restricted to relatively low contents. In EAF steels, scrap with low phosphorus levels is chosen when low-phosphorus steels are produced. While in general steels require a maximum of 0.03%, press hardened steels required a limit of 0.02% with an aim at 0.01%. Phosphorus is not eliminated during the DR process and hence the quantities found in DRI are directly a



function of those contained in the iron ore. Phosphorus content normally found in DRI ranges between 0.01 % and 0.04 %. The EAF process can be designed to favor dephosphorization: lower temperatures, high slag basicity, and high oxidation of the bath. However, P can be reduced by 20 % to 50 %. No further refining is possible by secondary metallurgy [ISPAT].

There is a higher level of S in the furnace charge than what is required in the final steel product so it needs to be removed. In the EAF. The conditions favorable for removal of P are the opposite of those necessary for the removal of S which becomes difficult and desulfurization during secondary metallurgy operations becomes a better option. Depending on secondary metallurgy practices on the sulfur level after EAF process leading to values varying between 0.006% down to 0.001%. [Mincu 2013]

S has an adverse effect on processability and product properties. In normal steels, Mn contents are high enough ( $Mn/S > 8$ ) to prevent pronounced segregation promoting granular weaknesses and cracks during solidification this problem. Thus, S appears in the microstructure as MnS inclusions that can act as stress raiser in steel products. Their shape and orientation give the steel a characteristic texture. For ultrahigh strength press hardened steels the sulfur risk is currently limited by a maximum content defined as 0.003% aiming at 0.015%. Under these conditions, the role of secondary metallurgy technologies and operations downstream to EAF become critical.

The replacement of a standard BOF steelmaking route for one consisting of EAF 100% Scrap involving a low level of CO<sub>2</sub> emissions introduces an important increase in residual elements (Cu, Sn, Ni) and nitrogen (N) contents with P remaining low and S being dependent mostly on the secondary metallurgy technology associated to the EAF. An increasing share of DRI beyond 50% in the EAF feedstock can lead to lighten these harmful effects by limiting the increase in the level of residual elements and nitrogen contents, with a risk of slight increasing P contents depending on the iron ore source. The DRI solution may represent however an increase in cost and CO<sub>2</sub> emissions.

To complete this phase the press hardened blanks will be characterized regarding basic characteristics of microstructures and in-use properties using standardized techniques, notably tensile testing (ISO6816) and bending tests (VDA238).

## 2.3 Tramp Element Segregation

The different Tramp Elements present in recycled steel distribute in preferential manners and locations [Calvo-Muñoz 2006]. While some remain homogeneously distributed in the matrix, others (again, notably Cu or Sn) segregate into grain boundaries or free surface, sometimes reacting with other alloying elements.

### 2.3.1 Grain Boundary (GB) Segregation

Grain boundary cohesion or strengthening plays a key role on the resistance of high strength steels to embrittlement. The segregation of impurities to GBs has been shown to dramatically alter the cohesion of GBs.

Regarding the segregation of impurities, from experiments it was demonstrated that it occurs within a few atomic layers at the GB plane. Rice and Wang proposed a thermodynamic model for intergranular fracture under constant solute concentrations, wherein the reversible effect of separation and the cohesive energy of GB vary linearly with the GB coverage [Rice 1989]. According to their theory the potency of an impurity in inducing the work of brittle boundary separation is a linear function of the difference between the segregation energies for the impurity at a grain boundary and the free surface; two new surfaces are formed during the fracture of the grain boundary (2gint). The results of the presence of segregants phosphorus, tin, antimony and sulfur in the ductile- brittle transition temperature of steel satisfied the hypothesis: each 0.1 J m<sup>-2</sup> reduction in 2gint due to segregation of solutes increases the





DBTT by the order of 60 to 80 K. These surfaces are characterized by the corresponding chemical potential and consequently, the Gibbs energy of the surface segregation. The segregation energy of each element could be effectively explained by the elastic energy derived from the difference in atomic radii between the host metal and solute element.

The origin of interstitial impurities embrittlement was discussed intensively in the literature [Weng 2001] but it remains under debate up to now. It is believed that the loss of hybridization between the GB atoms in presence of an interstitial impurity atom may reduce the cohesive energy and increase the chemical activity of the GB [Erbehart 1987]. Wang et al. extended the classical model for calculating the ideal work of separation and concluded that the intergranular failure occurs as a result of a reduction in the cohesive energy due to the solute atoms but with contributions from the structural and compositional changes in the GBs. The segregation of elements to GBs in alloys is complex, requiring careful consideration of the interplay between various effects. These effects range from those arising due to differing elemental behaviours, the chemical interactions with other segregating solutes, or distinct GB characters (i.e. local atomic geometry). The solute-solute interactions between segregating atoms at GBs are known as co-segregation effects. Such interactions can play a significant role in GB segregation behaviour, well reflected by the focus on such effects in steels for important solutes or impurities such as H [Biereis 2017], B and C [Yamaguchi 2011], Zn [Scheiber 2020], and P [Yamaguchi 2007]. The cumulative effect of impurity on the GB cohesion was studied in few papers only [Tahir 2014].

Theoretical studies of an interstitial impurity interaction with Fe GBs are mainly limited to the  $\alpha$ -phase and magnetism was not included often in calculations. On the other hand, few studies have analyzed the grain boundary segregation in  $\gamma$ -Fe owing to the difficulty of handling paramagnetism [Yamaguchi 2007]. As a result, there is little experimental data on the grain boundary segregation of various alloying elements at these grain boundaries [Biereis 2017] and insufficient knowledge to control it.

In actual conditions in martensitic steels, it has been reported that during austenitization, the solute element segregates to the prior austenite grain boundaries and tends to weaken or strengthen them. During quenching and subsequent tempering at relatively higher temperatures, segregation occurs along the martensitic interfaces introducing additional interfaces, leading to changes in ductility [Kazuma 2022].

Figure 2 shows the embrittling effect of individual solutes on grain boundaries of bcc iron. B, C, N, and the transition metals of groups 4 (Ti, Zr, Hf), 5 (V, Nb, Ta), 6 (Cr, Mo, W), 7 (Tc, Re), 8 (Ru, Os), 9 (Rh, Ir) and 10 (Ni, Pt) except Mn, Pd and Co strengthen the grain boundaries of bcc iron [Kulkov 2018]. It can be noted that most residual elements associated to EAF processing route contribute to grain boundary embrittlement: Cu, Sn, Sb, As, P, S along with H. The zone of segregation trapping due to the presence of the GB extends no more than  $3^\circ$  normal to the interface plane, beyond which no significant segregation effects are observed.

- S and P: Sulfur and phosphorous are embrittlement elements in Fe [Komazazki 2003]. It was established that the metalloid impurities forming isotropic polar-like bonds cause interfacial embrittlement and also break the mirror symmetry of the GB.
- V, Cr, Mn, Pd, Mo, Cr: It was reported that Mo, V, Cr introduce beneficial effects on the GB cohesion thereby improving its crack resistant properties [Lee 1984] whereas the reverse effects were obtained by Pd, Mn and Cu [Weng 2001].

X.He et al [He 2017] studied the energy associated with various elements (P, Cu, Ni, and Mn) at substitutional positions to the four  $\langle 100 \rangle$  and six  $\langle 110 \rangle$  symmetric tilt grain boundaries in BCC Fe. From Figure 3, the results indicate: 1) The binding energy of a substitutional P, Cu, Ni and Mn to the GB core is essentially determined by the structure of the GB interface. The energy calculations indicate that P and Cu have a detrimental effect on the GB cohesion, which will lead to GB embrittlement. This was confirmed in the work by Mai et al [Mai 2022] studying four GBs: “twin-like/stacking fault” ( $3(1\bar{1}2)[110]$ ), typical high-angle “coincident

site lattice"-  $(3(1\bar{1}1)[110], \bar{1}1(3\bar{3}2)[110])$  and one that possesses characteristics of a low-angle tilt GB  $(9(2\bar{2}1)[110])$ . They confirmed that Mo and W are strong cohesion enhancers for all studied GBs, Ni can act as either a GB cohesion enhancer or an embrittler, depending on the GB and Cu is an embrittler across all GBs studied [Mai 2022]. The GB character not only affects the segregation tendencies of the transition metals, but also the induced cohesion effects. The cohesion of the twin GB is significantly higher compared to the other GBs as they closer resembles the bulk structure. However, it is also substantially more vulnerable to Cu embrittlement. Both the "high-angle" coincident site lattice GBs possess similar  $W_{sep}$  (Work of Separation) as pure GBs, but exhibit vastly different potentials for strengthening via segregation engineering for certain solutes

The interactions between the Ni-Cu pairings in the GB needs to be also considered as it results in extraordinary attraction behaviour resulting in segregation binding. This example demonstrates the importance of explicit and thorough treatment of co-segregation effects. These interactions can vary wildly as a function of GB character and position. So, although there is relatively good overall qualitative agreement for the nature of solute-solute interactions at the bulk and GB, this is a dangerous quantitative extrapolation to make in modelling GB co-segregation, due to the nature of unique local GB atomic environments substantially altering interaction behaviours [Mai 2022].

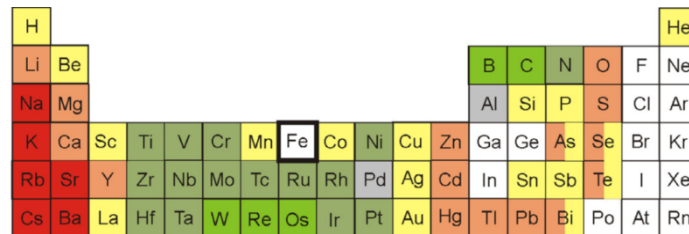


Figure 2: Character of individual solutes with respect to the strengthening and embrittling of grain boundaries in bcc iron. Elements marked by green shadows strengthen the grain boundaries in iron, elements marked by red, brown and yellow shadows embrittle them and those marked in grey are indifferent. Red:  $\Delta E_{SE,I} > 200$  kJ/mol, brown:  $200 > \Delta E_{SE,I} > 90$  kJ/mol, yellow:  $90 > \Delta E_{SE,I} > 10$  kJ/mol, grey:  $\Delta E_{SE,I} \approx 0$ , dark green:  $10 > \Delta E_{SE,I} > 100$  kJ/mol, bright green:  $\Delta E_{SE,I} < 100$  kJ/mol, striped brown/yellow: As, Se, Te and Bi are evident embrittlers but the values of  $\Delta E_{SE,I}$  were not presented till now. The effect of the solutes in white fields is unknown. [Kulkov 2018]

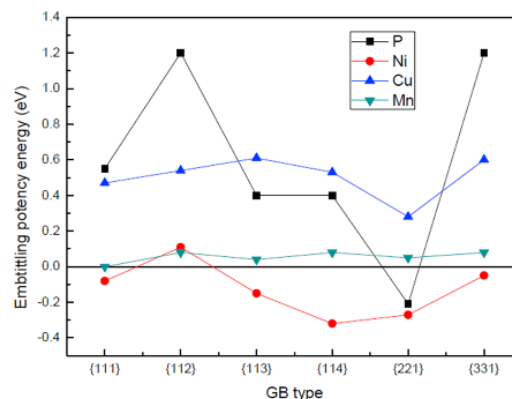


Figure 3: Embrittlement potency of P, Cu, Ni and Mn in bcc Fe [He 2017].

While Cu is soluble in austenite (up to 10wt%) its solubility in ferrite phase is much lower (up to 2.1wt%) and if Cu is kept in solid solution after cooling it can precipitate after tempering. It

is so far considered that fast cooling is not mandatory to keep Cu in solid solution as Cu diffusion is rather slow. When it occurs Cu particles are formed at grain boundaries beyond 5nm in size and not coherent with the matrix. The temperature range in which it precipitates is 400 to 700°C and C, Mn and deformation can accelerate the kinetics of precipitations. Guo et al [Guo 2019] reported on the grain boundary segregation of a hot rolled low carbon weathering steel containing 0.24%Cu with or without Sb additions considering a high angle grain boundary (45° misorientation). Figure 4 presents results of the APT study showing a reference of Cu segregation and precipitation to this grain boundary. It can be noted that Cu-Sb interaction led to Cu precipitation at the grain boundary.

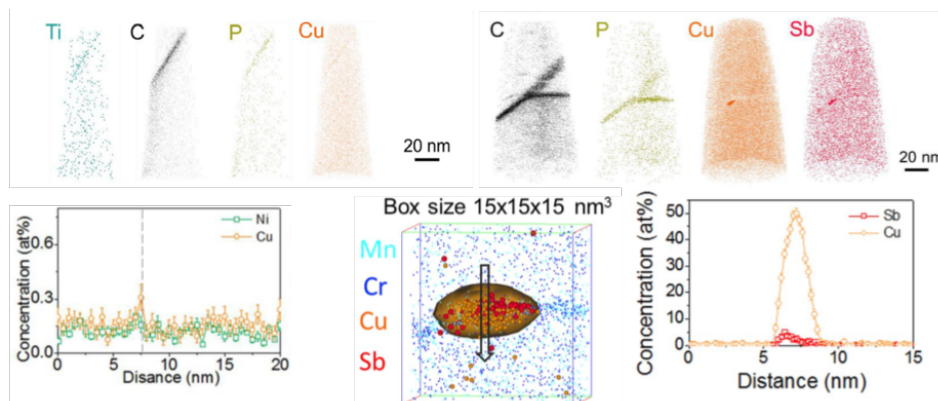


Figure 4: APT characterization of a GB of a hot rolled weathering steel containing 0.24%Cu [Guo 2019].

### 2.3.2 Surface Segregation

Surface segregation of an alloy is enrichment of the surface in one of the components in comparison to the bulk concentration. The driving force for this effect is the difference in surface energy between the constituent components of the alloy (whereby the component with the lower surface energy will tend to segregate to the surface) as well as the heat of solution of the minority element into the bulk of the majority component (whereby the component with a positive heat of solution will tend to segregate to the surface). Segregation also, is a manifestation of thermal and chemical equilibrium. Calculations of the strength of segregation can be attempted with simple models or models that are singularly complex.

Christien and Le Gall [Christien 2011] have studied the segregation of phosphorus in a martensitic steel comparing grain boundary and surface segregation during tempering treatments at 450, 550 and 650°C by Auger Electron Spectroscopy. The results shown in Figure 5 indicate a very fast phosphorus segregation on the surface; the apparent phosphorus diffusion coefficient worked out from the experimental segregation kinetics is 500 to 1000 times as high as the phosphorus bulk diffusion coefficient, which indicates a substantial contribution of phosphorus diffusion along the former austenitic grain boundaries. The phosphorus grain boundary concentration at the end of the Auger experiments was in all cases far from equilibrium.

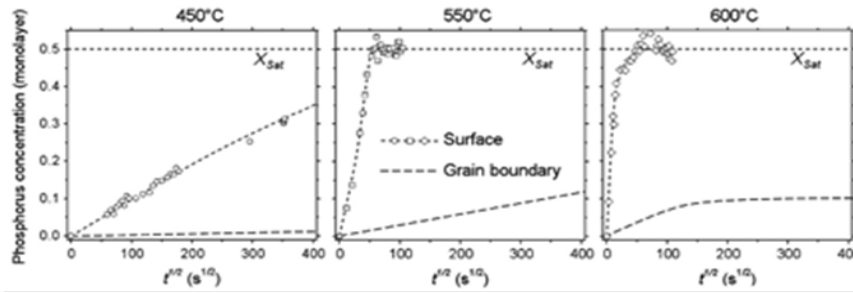


Figure 5: Kinetics of phosphorus surface and grain boundary segregation in a martensitic steel [Cristien 2011].

Regarding residual elements, Petrovic et al [Petrovic 2006] reported on the combined surface segregation of the impurity elements Cu, Sn, Sb, As and P in non oriented electrical steels in the temperature range from 50 to 900°C using Field Emission Auger electron spectroscopy to study the surface segregations. All these elements, although they are present in small concentrations they are very surface active. The Cu segregates to the surface of the steel at temperatures higher than 350°C. Its surface segregation depends on the temperature and the bulk concentration. The decrease in the intensity of Cu enrichment after 500°C is related to its desorption from the steel surface. There is a strong tendency for the surface segregation of Tin at higher temperatures while for P the peak is found at 600°C. Noticeably the surface segregation of As begins at  $T > 800^\circ\text{C}$ . These results reveal the strong tendency of residual elements for surface segregation under annealing conditions.

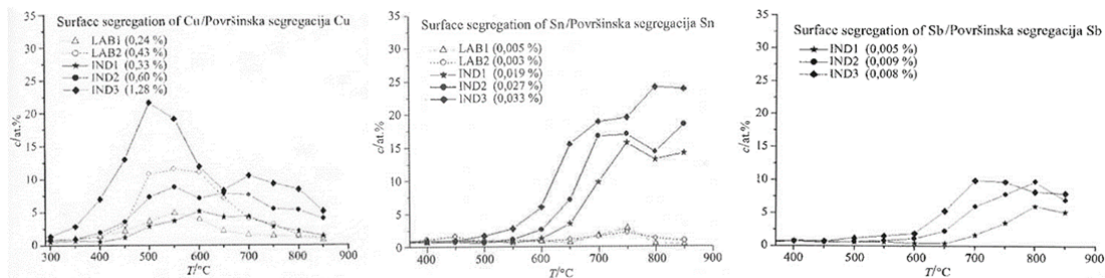


Figure 6: AES measurements on the surface segregation of Cu, Sn and Sb as a function of soaking temperatures for non-oriented electrical steels [Petrovic 2006]

Recent studies clearly highly that a high amount of elements (Cu, Sb, Ni...) can segregate and even lead to precipitation of Cu/Sb particles in the substrate [Zhang 2022]. The surface segregation is formed in the earlier stage of the steel processing during slab reheating and can remain at the until the end of the process, including on the final press hardened parts. The local consequences on the thermodynamics and phase transformation behavior of the AISi coating are so far absent in the literature.

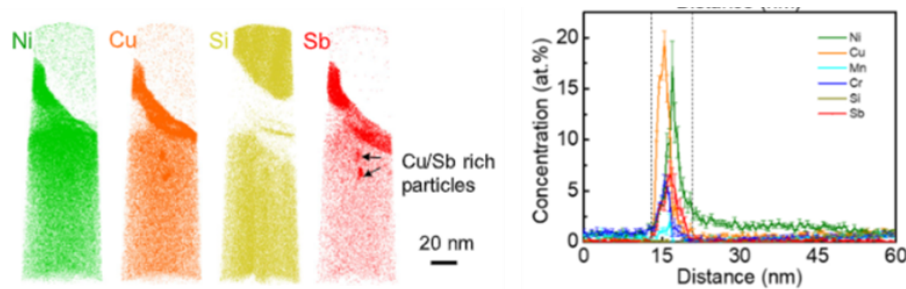


Figure 7: APT measurement of the surface segregation taking place in the earlier stage of the process (hot rolling) in a low carbon steel with a significant amount of residual elements [Zhang 2022].

The segregation of elements to GBs in alloys is complex and regarding the case  $\gamma$ -Fe in particular, which is the key domain in which segregation occurs in press hardening steels the amount of published research is rather limited. Moreover, the ultrahigh strength microstructures comprising exclusively or dominantly martensite present a large range of grain boundaries; from twin to high and low misorientations. As discussed above this further complexifies the segregations as many factors interplay. The co-segregation effects in the field of interest of this project have never been investigated, not only between the different residual elements Cu, Sn, Sb but also their interaction with P, H and B. Similarly, uncertainties arise regarding the cumulative effect of impurities on the GB cohesion as previous research is lacking.

## 2.4 Metallurgical Transformations Under the Effect of Tramp Elements

It is well known that B plays an important role as a hardenability agent in steels [Ueno 1988]. The advantages of B over the traditional alloying elements such as Cr, Mo, Mn, V, and Ni are its lower cost and a smaller quantity required for a remarkable hardenability in low-carbon alloys. For example, an addition of 20–30 wt ppm B to low alloyed steels provides the same effect on Improving hardenability as 0.4–0.7 wt%Cr, 0.3–0.5 wt%Mo, 1.0wt% Ni, 0.2wt%Mn, or 0.12wt%V. There as on for the enhancement of hardenability is that B can retard the austenite to ferrite and Pearlite transformation, thus enabling the martensite formation [Mun 2012].

The effect of B on suppressing the ferrite formation is proposed to be due to non-equilibrium segregation of B at prior austenite grain boundaries (PAGBs) during cooling [Asahi 2002], which may reduce the grain boundary energy, and thus the efficiency of the PAGB to support heterogeneous nucleation of ferrite. Different from the equilibrium segregation [McLean 1957] which is driven by the difference in free enthalpy of solute atoms in the matrix and at interfaces, the non-equilibrium segregation is associated with the formation of a large vacancy supersaturation and solute atom–vacancy complexes during cooling from high temperatures. Since grain boundaries (GBs) act as sinks for vacancies, a vacancy concentration gradient appears between GBs and the inner grain volume. Driven by the vacancy concentration gradient, solute atom–vacancy complexes diffuse towards GBs, leading to segregation of solute atoms at GBs. As the austenitization temperature and the cooling rate determine the vacancy concentration and its gradient, the magnitude of non-equilibrium segregation strongly depends on these two processing parameters [He 1989].

Besides the above-mentioned processing conditions, alloying elements also influence the B segregation behavior at PAGBs and hence the hardenability of steels. For example, an addition of Nb or Mo [Hara 2004] to B-added low carbon steels can additionally enhance the

hardenability of steels, whereas an addition of Cr has a smaller effect than Nb and Mo [Hara 2004]. Recently, Han et al. reported that the synergistic effect of the combined addition of alloying elements with B on the hardenability of steel depends on the cooling rate [Han 2008] and associated with the cooling rate-dependent segregation behavior of B at PAGBs.

Li et al [Lin 2015] reported on the site-specific preparation of APT tips containing a prior Austenite grain boundary was applied to study the segregation behavior of B and other alloying elements such as C, Mn and Si in a Quenched Cr-added Mo-free martensitic steel. Segregation of B at the PAGB and its absence at the M–M boundaries indicate a non-equilibrium mechanism controlling the B segregation behavior by forming mainly B–vacancy complexes. Figure 8 shows the APT element maps illustrating the contrast between PAGs and M-M boundaries.

However, the state of the art lacks description on the interaction of B with residual elements on grain boundary segregation and its effect on phase transformation and hardenability. All these aspects are pivotal in the use case of Boron Steel.

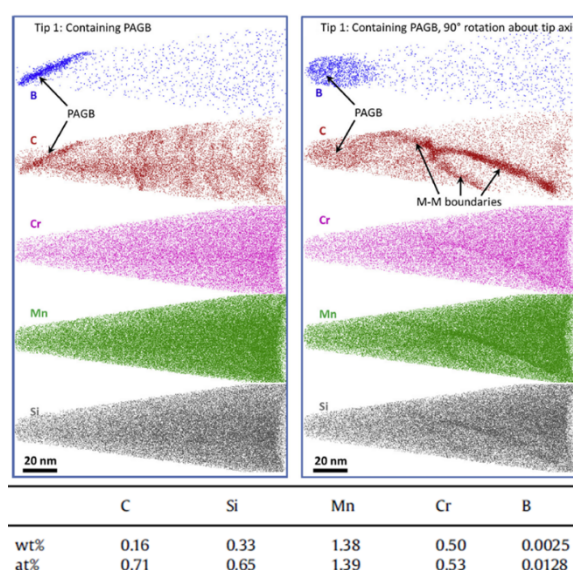


Figure 8: 3D Atom maps of the as-quenched martensite and chemical composition of the studied grade [Lin 2015].

## 2.5 Effect of Tramp elements on Ductility and Fracture Behaviour

Residual elements can induce embrittlement due to grain boundary segregation. An important related aspect is the ability of the elements to reduce grain boundary (GB) cohesion. It was calculated that the grain boundary cohesion in ferrite is reduced in proportion to the excess size of the segregated atoms (see Figure 9 left) [Rod 2006]. This reduction of GB cohesion makes fracture more likely. It can be observed as a decrease of the absorbed energy (see Figure 9 right) and/or increasing the transition temperature (TT) [Materkowski 1979]. Residuals such as Sn, Sb, As and P increase the TT, whereas Be, C and B decrease it [Rod 2006]. The latter is extremely relevant as elements such as Sn, Sb, As and P are highly likely present in important amounts in the steel when using low CO<sub>2</sub> steel processing routes.

Temper Embrittlement (TE) is associated with tempered alloy steels that are heated within, or slowly cooled through, a critical temperature range, generally 300 to 600 °C [ASM 1996]. This phenomenon is of primary interest for PHS as Die-Quenching is characterized by slow

cooling rates in the aforementioned range of temperatures and more innovative hot-stamping processes as “multistep” will also cover this range of temperatures with an increased risk of TE. Temper embrittled steels exhibit an increase in their DBTT and a change in fracture mode in the brittle test temperature range from cleavage (or quasi-cleavage) to intergranular decohesion, essentially along prior austenite grain boundaries [Guttman 2001]. It occurs only in alloy steels, not in plain carbon steels, and the degree of embrittlement varies with alloy steel composition [ASM 1996]. Therefore, the alloying elements present, and their combinations and levels, are important. Impurities, in decreasing order of influence in terms of weight percent, are antimony, phosphorus, tin, and arsenic [ASM 1996]. Nevertheless, their segregation and therefore their influence on embrittlement will vary with microstructural features as grain size and interactions with alloying elements (e.g., solubility effects and competition for available grain boundary sites) [Guttman 2001]. Empirical relationships exist in the literature to predict the influence of residual elements on the sensitivity of steels to Temper Embrittlement such as Bruscato (1970) and Watanabe (1982).

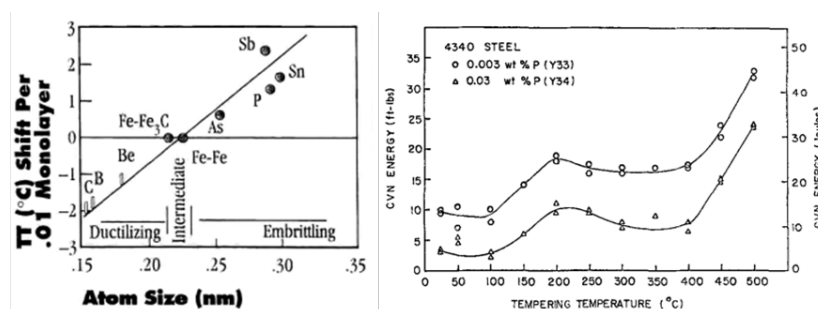


Figure 9: left: relation between atom size of residual elements and embrittlement (transition temperature shift) [Rod 2006]. right: room temperature Charpy impact energy vs tempering temperature for 4340 steel [Guttman 2001].

## 2.6 Effect of Tramp Elements on Formability

Several studies exist linking the formability of sheet metal to the presence of inclusions or unwanted phases; this is particularly relevant in a scenario where circular economy and recycled metal need to be massively deployed into the market. Use case examples, such as [de Caro 2023 and Poole 2011], showcase this behaviour for steel and aluminium alloys.

In the case of press hardening steels, room temperature formability is not particularly important – high temperature formability, on the other hand, becomes extremely important. And, again, this becomes related to the effect of grain boundary segregation.

Hot stamping takes advantage of the hot ductility of the austenite phase to produce complex shape that would not be achievable with a 1500-2000MPa martensitic grades with cold forming. The typical maximum local strain applied during forming process is typically around 0.2; beyond this value, hot stampers may encounter local thickening, thinning or failure of the part. To assess the feasibility of a part, finite element modelling is performed considering extrapolated hot Forming Limit Diagram at the coldest point of the forming (between 600 and 800°C). To calibrate the model required to have the virtual FLD, several mechanical tests are performed such as hot tensile test or hot Nakajima / Marciniak tests [Georgiadis 2017]. Naturally, there is a decrease of ductility when lowering the forming temperature, but additional phenomena can take place during the process and could lower the formability such as grain boundary embrittlement or phase transformation.

High temperature segregation can take place at the so-called Prior Austenite Grain Boundary during the austenitization and during the highest temperatures of the die quenching (at lower temperature the diffusion is not fast enough to allow the onset of the segregation). The modification of the local equilibrium existing at the PAGB can either lower the toughness of the hot steel or promote the formation of ferrite leading to weak ferrite/austenite interface at high temperature (hot ferrite having a lower ductility than hot austenite at a given temperature). The presence of residual elements such as Sn or Sb at the PAGB can modify the amount of B segregated [Peng 2015]; elements which play an important role for both, the hot ductility and delayed austenite transformation as shown in Figure 10. The presence of Cu is also reported to create a loss of hot ductility [ASM 1996] typically in the range of hot forming temperature used in hot stamping. This loss of ductility is observed on hot tensile specimen by analyzing the Reduction of Area which traduces the ability of the material to sustain local deformation.

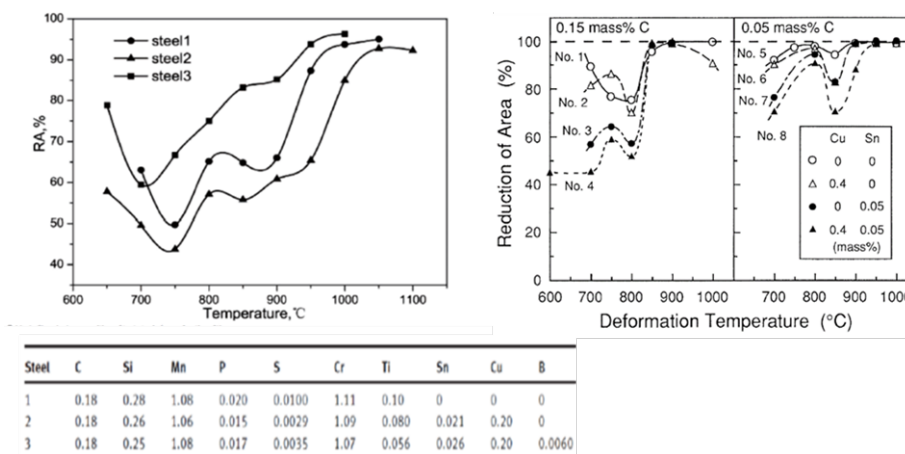


Figure 10: Loss of hot ductility emphasized by the presence of Cu and Sn in the range 600-800°C for low carbon steels [Peng 2015- Matsuoka 1997].

## 2.7 Hydrogen Embrittlement on Tramp Element-Containing Steels

The increasing demand for ultrahigh-strength steel for automotive steel sheets has challenged developers as with higher strength levels, the susceptibility to hydrogen embrittlement increases. The risk of degradation of properties by the presence of hydrogen resulting in sudden and unexpected fracture is a factor that could limit its application. Notably, in martensitic press hardened high-strength steel parts, subjected to residual or assembly stresses cracking at the prior  $\gamma$  grain boundary could be triggered in hydrogen environments either associated to the part manufacture or to corrosion phenomena under service.

Two different mechanisms have been identified causing the hydrogen induced fracture of high strength steels. Beachem suggested that the presence of H may enhance the dislocation activity, thereby facilitating the formation of voids; in addition, their subsequent coalescence causes crack propagation, resulting in a transgranular failure with a dimple-like fracture surface, which is known as “hydrogen-enhanced local plasticity (HELP) mechanism” [Beachem 1972].

In contrast, it is widely known that H present in materials can result in a transition in the failure mode from ductile transgranular to intergranular due to the decohesion caused by H segregation at the grain boundaries (GBs) of high strength steels; this is known as “hydrogen-enhanced decohesion (HEDE) mechanism” [Vergani 2014]. Therefore, the relationship





between H trapping and H embrittlement has attracted research attention. Chen et al. provided the direct evidence for the dislocations and GBs acting as trapping sites [Chen 2020] and Martin et al. suggested that the accumulation of H atoms at the GBs of martensitic steels could induce intergranular failure in the stress strain behavior [Martin 2019].

Grain boundary cohesion or strengthening plays therefore a key role on the resistance of high strength steels to hydrogen embrittlement. The segregation of impurities to GBs has been shown to dramatically alter the cohesion of GBs. Grain boundary cracking in hydrogen environments is closely related to the grain boundary segregation of alloying and impurity elements at the prior  $\gamma$  grain boundaries. Because the grain boundary segregation state at the prior  $\gamma$  grain boundary is mainly determined in the  $\gamma$  region, controlling the grain boundary segregation in the  $\gamma$  region is important for improving the hydrogen embrittlement resistance of martensitic high-strength steels.

Recently published research work on the impact of increasing the P content from 0.01 to 0.02% in a 0.1%C DP steel clearly illustrate this sensitivity in High Strength Steels [Dong 2022]. In this work a DP steel having 75% martensite and 25% ferrite and tensile strength of 1180MPa was subjected to linear increase tensile stress with simultaneous cathodic charging of hydrogen. An increased P content led to a large reduction in ductility associated to enhanced the hydrogen-induced martensite related cracking. The role of the excess P content on HE susceptibility of DP steel could be summarized as: (i) the excess P content enhances element segregation (by both increased tendency of P segregation and promoted other element segregation like Mn); (ii) both the hydrogen-induced micro-crack initiation and the cracking propagation in martensite and at the interfaces are enhanced following the HEDE mechanism; the higher P solution content led to ductility loss in ferrite followed the HELP effect, decreasing the inhibit effect on crack propagation by ferrite deformation, enhancing HE susceptibility.

Hydrogen induced embrittlement risks in ultrahigh strength press hardened steels are threefold; i) the risk of delayed fracture occurring in parts after assembly when a critical combination of hydrogen content introduced during austenitization in the hot stamping furnace, applied assembly stresses and microstructure cohesive strength could trigger fracture; ii) the risk of ductility loss induced by the hydrogen content of the material when subjected to plastic deformation under assembly or crash conditions as a consequence of the weakening of grain boundary cohesive strength and ii) the risk of stress corrosion cracking occurring during the lifetime of the vehicle after a critical local combination of residual stresses in the part, microstructure cohesive strength and the hydrogen introduced by corrosion phenomena is reached.

## 2.8 Interaction of Tramp Elements with the Coating

The effect of residual elements segregated at the steel surface on the Al-9%Si coating after hot dip galvanizing has not been yet determined for press hardening steels. The surface reactions involved in the hot dip deposition of the Al-Si coating are known to involve a level of dissolution of the steel substrate. It is uncertain the effect of these reactions on the surface enrichment profiles of these elements. The hypothesis of an enrichment of the Al-9%Si coating with these elements cannot be neglected and therefore a role of these elements needs to be studied not only after hot dip galvanizing but also after austenitization treatment in hot stamping.

Regarding the hypothesis of enrichment of the coating in residual elements, the work recently published by Z.Xiong et al [Ziliu 2021] reports on the impact of Cu in the Al-10%Si coating of 22MnB5 grade. In this study the effect was studied for a nominal amount of Cu between 0.5 and 3% showing that may lead to the preferential formation Cu-Al rich phases in the free coating as well as in the interdiffusion layer. Cu seems to be preferentially distributed in grain boundaries as well as in coating surface after the galvanizing step. After the thermal

treatment, Cu tends to diffuse towards surface. As paint adhesion on AlSi coating is specially linked to its surface topography after PHS process, is it necessary to verify if Cu enrichment may change coating roughness as well as paint adherence. Figure 11 shows the chemical profiles of Al, Si and Cu before and after hot stamping clearly illustrating the diffusion of Cu into the coating during the alloying treatment.

Considering the hot stamping treatment, the presence of Cu leads to a decrease in solidus temperature down to 523°C from 575°C for standard AlSi coating. It could be argued that this decrease in melt temperature could enhance risks related to rolls build-up or die pollution during hot stamping process.

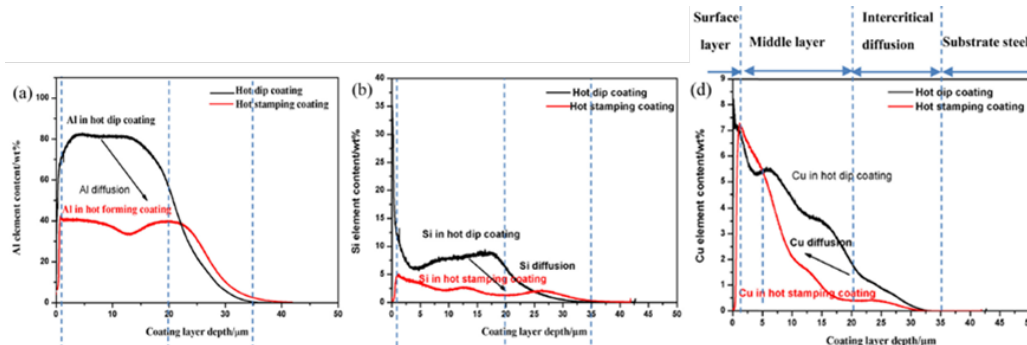


Figure 11: Al, Si and Cu distribution in hot dip and hot stamping coatings with the heating temperature of 850°C [Ziliu 2021].

No prior research has been published on the combined role of residual elements in the steel substrate in the nature and alloying of the Aluminium Silicon based coating.

### 3. Problems Encountered and Proposed Approach

#### 3.1 Definition of the Problem

##### 3.1.1 European Steel Industry towards Carbon Neutrality by 2050

Steel is one the most important engineering and construction materials, it is present in many aspects of our lives. The steel industry now needs to transform in order to reduce its carbon footprint from both environmental and economic perspectives. Currently the steel industry is among the three biggest producers of carbon dioxide, it accounts for 7-9% of global carbon emissions [ArcelorMittal 2021]. The transition to carbon-lean, 'green' steel requires a fundamental change in the way steel is made, because our current processes are already at the technical and thermodynamic limits [Eurofer 2020]. The European steel industry is committed to meeting a 30% reduction in greenhouse gas emissions by 2030 and carbon neutrality by 2050 while keeping 330000 direct jobs and 160 Mt of steel production in Europe [Eurofer 2020].

Short-term CO<sub>2</sub> emissions reductions in the European steel sector has at its core the transition to Scrap-based steel production. However, longer-term reductions will require the adoption of new direct reduced iron (DRI) and smelting reduction technologies that facilitate the integration of low-carbon electricity (directly or through electrolytic hydrogen) and Carbon Capture – Utilisation and Storage (CCUS), as well as material efficiency strategies to optimise steel use [Vass 2021].



Scrap-based steel production is considerably less energy-intensive than primary production from iron ore. Scrap is used as the main ferrous feed in electric arc furnaces (EAFs). Scrap-based production in EAFs accounted for just about 20% of production in 2020. As a small share of Scrap is also used with ore-based inputs in blast furnace-basic oxygen furnace (BF-BOF) production the current scrap inputs account for ~30% of total crude steel production [Vass 2021] The overall availability of scrap is limited which is a key constraint for largely extending its use in steel production. To get on track with the carbon neutrality scenario by 2050, the global market share of scrap-based production by EAFs needs to reach over 27% by 2030 and scrap inputs should account for close to 40% of total crude steel production.

Emissions can nevertheless be reduced in the short term by increasing gas-based DRI production, which is less emissions-intensive than coal-based BF-BOF production and currently accounts for about 5% of steel production and planned to reach 8% by 2030 [Vass 2021].

### 3.1.2 Materials Production: a new challenge in the race to the Zero Footprint Car

The automotive industry contributes over 10% of industrial emissions responsible for global warming. The sector must also embrace life cycle decarbonization. 65-80% of life-cycle emissions of a standard Internal Combustion Engine Vehicle (ICEV) come from its exhaust emissions. Hence, until recent years, automotive decarbonization has been focused only on electrifying powertrains, optimizing them, and making greener the energy mixture to power them to significantly reduce use-phase emissions [McKinsley 2020]. However, electrification is not the unique answer. The automotive industry had also to start tackling emissions embedded in vehicle materials. To date, vehicle materials already account for ~18-20% of life-cycle emissions of ICEVs. With the increase of powertrain electrification (Electric Vehicles (EV)) the importance of life-cycle emissions of materials will increase too and could achieve more than 60% by 2040 if it is not reduced [McKinsley 2020]. The latter will shift the balance of the automotive sector's carbon footprint to materials production creating a new challenge in the race to the true zero footprint car.

### 3.1.3 Press Hardening Steels providing safety and lightweight potential have become key automotive materials

The automotive sector represented in Europe 16% of total finished steel products in 2021 with Construction sector amounting to 37% Today's car bodies have to meet various different and partly contrary requirements in the automotive industry. Higher demands on passive safety tend to result in weight increase while ecological aspects like reduction of fuel consumption and carbon dioxide emission call for light weight constructions. The application of high strength steels was the first answer to ensure the required safety directives in a light weight car body construction. Although high strength steels have superior mechanical properties, stamping operations become more difficult. High strength goes parallel with reduced formability, increased spring back behavior and excessive tool wear in cold forming applications.

Press hardening steel has become a much-used material in car body manufacturing due to its excellent safety and lightweight potential. In some recent car models press hardening steel has reached already a weight share by more than 20% in the body structure while it is estimated that it could reach even around 40% in the future.

Market needs for press hardened steels worldwide currently exceeding 3MTon of which more than 1MTon is produced in Europe exclusively using blast furnace-basic oxygen furnace (BF-BOF) production. The utilization of hardenable steel in combination with press hardening applications began in the 1990s but its application worldwide had a sharply increase in the last 10 years [HSSinsights].

Press hardening steel is mainly used for producing passive safety components. Hot-formed grades currently present in the market cover two key safety functions: a) anti-intrusion parts for which an ultimate load before collapse is required and b) energy absorption parts which



need to absorb energy during an impact. Usibor® ultrahigh strength steels (TS 1500 to 2000MPa) provide anti-intrusion solutions while Ductibor® (TS 450 to 1000MPa) are focused on energy absorption applications [ArcelorMittal2]

The most widely applied solution is Usibor® 1500 a 0.22%C Boron steel of grade 22MnB5. The typical parts in the Body-in-White supplied with press hardened steels: front and rear bumper beams; Door reinforcements; Windscreen upright reinforcements; B-pillar reinforcements; Floor and roof reinforcements; Roof and dash panel cross members. Its main advantages are its ability to achieve complex geometry by forming in austenitic state, total absence of springback, uniform mechanical properties obtained on the part, exceptional fatigue strength and impact resistance, allowing substantial weight reduction.

This solution is supplied with an Al-Si coating obtained by continuous hot dip galvanizing. Originally designed to protect it against oxidation during the forming process; the corrosion resistance of this coating has been demonstrated in a variety of atmospheric corrosion tests enabling 15-year service life to be attained for the most severe automotive applications [7]. Typically, the Al-Si coating has a nominal thickness of 30-50 µm, a basic composition 90 % Al + 10 % Si with Si enriched locally. The interlayer at the interface with the steel substrate formed by the heat treatment (forming process) has a thickness of 5 to 10 µm. Its basic constituents are FeAl and Fe<sub>2</sub>Al<sub>5</sub> phases.

In the hot stamping process this hardenable boron steel (between 0.002% and 0.005% boron) is austenitized at a temperature above 850°C and then quenched between cold tools with cooling rates greater than 25 K s<sup>-1</sup> to attain martensitic transformation. This process applied on AS coated press hardening solutions presents several advantages: a simplified process and cost savings, elimination of the shot-blasting step (no formation of scale), no need for protective atmosphere in austenitization ovens, excellent temporary corrosion resistance after stamping, no need to oil parts before assembly, no decarburization and excellent resistance to pitting corrosion. Most important, the carbon footprint of this stamping process remains negligible compared to the benefit of the reduced material engaged (lightweight).

#### 3.1.4 Low CO<sub>2</sub> Press Hardened Steel production introduces high content of residual elements

The use of EAFs allows steel to be made from a 100% scrap metal feedstock and residual elements are unwanted alloys that occur in scrap. These elements are Cu, Sn, Sb, As, Ni, Mo, Cr and can reach cumulative contents beyond 0.3w% more than 3 times that typically obtained in BOF steelmaking routes. Moreover the EAF route involves also variations in key elements such as P, S and N.

Residual elements are known to significantly affect grain boundary and surface segregation phenomenon leading to embrittlement

Residual elements have a strong tendency to segregate to grain boundaries and surface of steel and locally their composition can increase dramatically depending on the element, the nature of the boundary, the thermomechanical treatment conditions to which the steel is subjected and the presence of other segregating elements. Most of the residual elements Cu, Sn, Sb, As and also P and S when segregated to grain boundaries bring a decrease of the cohesive strength of boundaries in the steel microstructures and this is directly linked to a decrease in toughness and the resistance to embrittlement.

Grain Boundary and Surface Segregation are Key Factors in Press Hardening Steel Performance

In standard press hardened steels the final microstructures are formed by die quenching of austenite to form martensite and/or martensite/bainite mixtures and segregation phenomena in the prior  $\gamma$ -phase occurring during the austenitization treatment are already key factors in the press hardening steel performance. A main requirement of press hardening steel design



is the capacity to inhibit the ferritic transformation during cooling first in air at the exit of the furnace and after during quenching in the die. To ensure this required hardenability B additions are made at the level not exceeding 30ppm as it is known that B segregation to austenite grain boundaries strongly delay ferritic and bainitic transformations. Moreover, the press hardening material is hot formed in the austenitic phase at the temperature range between 600 and 750°C. Hot formability is therefore a key requirement of this product family and factors affecting high temperature embrittlement are needed to be carefully managed to ensure applications according to OEM part design requirements. Another significant aspect to be considered is that of hydrogen absorption that occurs in the steel during the austenitisation treatment with hydrogen being introduced after dissociation of the water molecule adsorbed at the surface of the steel coming from unavoidable humidity in the furnace air based atmosphere. Hydrogen diffuses into the austenitic matrix favored by its rather high hydrogen solubility. After quenching and the martensitic transformation hydrogen atoms are distributed among many microstructural features acting as trapping sites, most notably prior austenite grain boundaries and dislocations which in turn transport hydrogen atoms to grain boundaries when external stresses are applied. Hydrogen present in the steel with contents not exceeding 0.5ppm becomes one of the most potent grain boundary embrittling elements and the press hardened steel design requires particular attention to grain boundary cohesive strength to counteract this effect. Finally press hardening solutions are mainly constituted by ultrahigh strength steels with strength levels from 1500MPa and beyond 1800MPa. As embrittlement sensitivity is known to sharply increase with material's strength, this positions the press hardening steels under a critical condition requiring control of factors affecting grain boundary strengthening. The introduction of residual elements in these solutions potentially affect each of these key aspects of press hardening steel behavior.

### 3.1.5 The Impact of residual elements on press hardening steel product requirements is uncertain and could limit the potential of CO2 emission reductions if not mastered

The combined effect of residual elements segregated to grain boundaries and surfaces in ultrahigh martensitic press hardening steels has not yet been determined and research references are mostly associated to segregation in  $\alpha$ -Fe rather than austenite. No research has been published on the interactions between B segregation and residual elements in austenite under conditions of hot stamping combining the effect of cooling rates and deformation. These phenomena could be potentially damaging for the high temperature formability of press hardening steels. No research work has been focused on the link between combined grain boundary segregation of solute elements and hot ductility in B steels. Hydrogen enhanced decohesion (HEDE) mechanism is considered the dominant embrittlement mechanism in ultrahigh strength martensitic steels triggering intergranular fracture. While this subject has been the focus of intense research, no reports have been published on the combined role of residual elements Cu, Sn, Sb on the sensitivity to hydrogen embrittlement. Grain boundary embrittlement is a complex phenomenon involving a large number of parameters. Moreover, its characterization requires advanced techniques such as atom probe tomography. These factors have limited the experimental work on this subject in ultrahigh strength steels that has now become vital in the context of the transition of steelmaking practices towards electric arc furnace and increasing use of scrap as source. In a similar way the surface segregation phenomena require detailed research in these steels that are sensitive to the nature of the surface not only in terms of coating performance but also in terms of the nature of the subsurface layer.

Considering the aforementioned, COOPHS project addresses the impact of low CO2 steel processing routes on the performance of ultrahigh strength press hardened steels and the development of a methodology to optimize the compromise between CO2 emissions and product application requirements. The knowledge gathered is expected to advance the state of the art about the impact of residual elements in press hardening steel products to boost the production and utilization of low CO2 steels in the automotive industry.



## 3.2 COOPHS Approach

As described in the proposal, the project is structured in 5 Phases – these phases have been designed to tackle the issues identified in the State of the Art in order to accomplish the objectives of the project.

### 3.2.1 Phase 1: Steelmaking including Residual Elements

**Phase 1** addresses the steelmaking itself, and producing the material that will be used through the project.

As discussed in section 2.1, scrap-based steelmaking introduces undesired trace elements in the steel composition. This is particularly true if scrap loads are maximized, which is the desired scenario.

Out of these elements, Copper plays a protagonist role. Cu remains in solution during the melting, and does not significantly react into the scrap. Current BOF-based high performance steels limit copper in the 0.03 % range, reaching 0.08 in some cases. However, post-consumer scrap reaches levels of up to 0.3 % Cu [BDSV 1995, Dworak 2021]. Cu is compounded with Sn, with similar overall effect in terms of ductility reduction.

Nitrogen is also introduced in the EAF, in much higher proportion than in BF/BOF. This can be an issue in Boron steel, due to possible reaction between B and N in solution. While this can be compensated by Ti, this leads to the formation of TiN precipitates.

Other elements that don't react into the slag include Ni, S and P. Ni has overall beneficial effects, and the amount present in scrap is not significant enough to cause problems, while S and P can be eliminated by already existing techniques.

Therefore, **this Phase 1 is focused on the production of thin gauge (~1.5mm) press hardened material of grades TS1500 to TS1800MPa having a large scope of chemical composition variations in terms of residual element contents** (mainly Cu, Sn, Ni, N, S, P). These chemical composition variations are representative of steelmaking production routes with different levels of CO<sub>2</sub> emissions in terms of kg CO<sub>2</sub>/Tn steel. Casts will be produced with an “artificially introduced” amount of residuals, to generate different scenarios comparable to scrap-based steelmaking.

In this project two steel grades were selected: 0.22%C and 0.34%C grades aiming at final press hardening product of TS1500 and TS1800 respectively. While TS1500MPa is the most widely applied press hardened steel grade for safety parts in automotive with high resistance to intrusion under crash conditions; TS1800MPa was selected as it represents the grade of maximum strength currently applied in anti-intrusion application in the vehicles. It is well known that toughness and embrittlement resistance tend to be increasingly affected as the level of strength of the material increases.

Regarding the residual element contents this project aims at studying a range between a minimum value representative of current standard BOF steelmaking routes with residual elements RE (Cu+ Ni+ Sn+ Sb +Mo) 0.05% / Nitrogen 30ppm / Phosphorus 0.010% / Sulphur 0.0015% to a maximum representative of EAF steelmaking route with 100% low Quality Scrap Charging consisting of residual elements RE (Cu+ Ni+ Sn+ Sb +Mo) 0.25% / Nitrogen 100ppm / Phosphorus 0.025% / Sulphur 0.0035%.

This first phase combines industrial and laboratory production of cold rolled and annealed & aluminized thin gauge material in order to cover both typical and extreme compositional changes.

Industrial Production Facilities: The key industrial facilities to be used in this phase for the production of cold rolled and annealed&aluminizing of the selected steel grades are: i) Fos-Sur-Mer plant of ArcelorMittal (France) with a standard BOF route with secondary metallurgy technology consisting of Ladle Furnace and Vacuum degasser. This plant will supply the



material in hot rolled coils using the industrial hot strip mill., ii) Sestao plant of ArcelorMittal (Spain) with EAF route with secondary metallurgy technology consisting of a Ladle Furnace. This plant will supply the material in hot rolled coils using the CSP compact strip mill technology. iii) Sagunto plant of ArcelorMittal (Spain) will focus on the pickling, cold rolling and annealing & hot dip aluminizing technologies available in this plant.

Laboratory Production Facilities: The key laboratory facilities to be used in this phase for the production of cold rolled and annealed&aluminizing of the selected steel grades are those at ArcelorMittal Maizieres Research (France): i) Vacuum Induction Melting (VIM) furnace to cast 60kg ingots of selected compositions, ii) Laboratory hot rolling mill (LTC), iii) Laboratory cold rolling mill (BHS) and iv) Infrared Furnace (IR) for annealing simulation.

Press Hardening Facilities: Press hardening of the above produced materials will be performed in a fully automatic semi-industrial hot stamping line at Gestamp laboratory (Sweden). The line has the possibility to vary furnace atmosphere depending on surface condition, AS coated or uncoated. In the case of standard press hardening flat water cooled dies will be used, and in the case of non-standard, 'bainitic', flat heated dies will be used.

Methodology for determining CO<sub>2</sub> emission levels: This calculation will be performed according to the Environmental Product Declaration for Recycled and Renewably Produced Hot Rolled coil production according to ISO 14025 and EN 15804+A1. The calculations include: i) The provision of resources, additives, and energy, ii) the Transport of resources and additives to the production site, iii) the Production processes on site include energy, production of additives, disposal of production residues, and consideration of related emissions, iv) Recycling of production/manufacturing scrap. Steel scrap is assumed to reach the end-of-waste status once.

### 3.2.2 Phase 2: Advanced characterization

Phase 2 is focused on the advanced characterization of the produced ultrahigh strength press hardened steel microstructures in terms of surface and grain boundary segregation. For this, materials containing different levels of residual elements content will be sampled and subjected to analysis at a nanometer and micron levels aiming at revealing the segregation of grain boundaries, surfaces and coatings, as pointed out in sections 2.3.1, 2.3.2 and 2.8.

The methodologies that will be used in COOPHS project to characterize surface and grain boundary segregation behavior of residual elements and their associated microstructural changes are described here below (from micro scale to nano-scale):

- Electron Probe MicroAnalysis – field electron gun (Feg-EPMA): is used to quantify the chemical composition across the thickness of the steel sheets at sub-millimeter scale. FEG-EPMA differs from conventional EPMA. It produces a narrow electron beam allowing for a highest spatial resolution. This technique is therefore ideal to have a global view of the through thickness heterogeneity.
- Glow Discharge Optical Emission Spectroscopy (GDOES): is used to study the chemical variation existing at microscale typically in multi-layer materials (such as Fe / Al coating interface). The plasma generated by the technique erodes, layer by layer, the metallic materials on a spot of few millimeters leading to a qualitative analysis of the elements present in the area. A semi-quantitative approach can be performed in a second stage with standardized specimen.
- Electron Backscattered Diffraction (EBSD): is used to characterize the crystallographic features of a microstructure. In martensitic steel, it allows for the characterization of the complex structure including packets, blocks, sub-blocks, laths. It also allows for the reconstruction of the prior austenite grain boundary before



- Focused Ion Beam milling of APT tips in the appropriate area (with the correct crystallographic characteristics).
- Dual beam SEM / Focused Ion Beam (FIB) / Transmission Kikuchi Diffraction (TKD): is used to nano-mill either the APT tips or the thin foils for TEM. A Gallium beam is used to shape the specimens using different patterns depending on the final shape expected.
  - Atom Probe Tomography (APT): is used to quantify at atomic scale the segregation taking place either at prior austenitic grain boundaries or at the Fe / Al interface. This advanced technique includes the quantification of the lightest elements (N, B, C...) which is difficult with other techniques. It allows for a 3D-representation of the atoms which have been evaporated from the tip milled with FIB.

### 3.2.3 Phase 3: Implications of Tramp Element Segregation on Metallurgy and Performance

Phase 3 is focused on identifying and quantifying the impact of increasing content of residual elements on the behavior of ultrahigh strength press hardened steels of grades TS1500 and TS1800MPa regarding key issues for process, product and application performance. The main aspects to be investigated are those related known to be affected by segregation phenomena: i) hardenability and interaction with B, ii) high temperature formability and ductility throat, iii) temper embrittlement and iv) hydrogen induced fracture behavior and interaction with Hydrogen trapping.

For the characterization of segregation, the following techniques have been proposed:

- Nano-Secondary Ion Mass Spectrometry 50 (nano-SIMS 50L): it will be used to localize and quantify the Boron segregation on prior austenite grain boundary (in parallel with APT). Compared to conventional SIMS, the nano-SIMS allows for achieving a finer lateral resolution. It is ideal to visualize the global behavior of the boron before APT, specifically to differentiate the presence of boro-carbide at PAGB from a local segregation. The equipment is available at the Luxembourg Institute of Science and Technology (subcontracted task by AMU).
- Advanced Microstructural Analysis FegSEM-TKD/TEM-ASTAR: it will be used to characterize the microstructure down to the nano-scale including the phase identification, the crystallographic orientations of these phases and their dislocations density.
- High energy X-Ray diffraction (Alba synchrotron): it will be used to follow in-situ the phase transformation taking place in the studied steels. It will be also used to follow the tempering kinetics including the carbide formation and the evolution of the dislocation density. This technique allows for an in-situ continuous characterization of the phase transformations under non-isothermal conditions. The approach was successfully used in the current RFCS-MiPRe project.

As a first subject of study, this segregation will have an impact on the **metallurgical transformations**, following section 2.4. This affects both the upstream processability of the material as well as its behaviour during press hardening. The project aims to address the topic through following methodology:

- Dilatometry: measures the volume changes related to phase transformations. It will be used to compare the modification of phase transformation kinetics relative to the presence of the presence of residual elements.
- Press Hardening: A press hardening parametric study will be performed in a lab-scale test setup at Gestamp laboratory (Sweden). The equipment to be used consist of a press equipped with a flat tooling for smaller coupons and batch furnace. The tooling has the capability to be used either with water cooling or with heating for standard and non-standard press hardening. The outcome will be evaluated through standard uniaxial tensile testing, to characterize the strength levels and strain





hardening curves, and through notched tensile testing, to quantify the necking and related strain at failure.

A second topic is how this tramp elements affect ductility, as described in section 2.5 and 2.6. This project aims to address the issue of temper embrittlement and low temperature ductility through the application of a complementary set of experimental techniques:

- **Essential Work of Fracture:** This method was developed by Cotterell and Reddel to quantify the energy per unit area consumed in the formation of two fracture surfaces in metal sheets. It has been recently adapted by EUT to the fracture toughness evaluation in AHSS sheets, and successfully applied in previous RFCS projects to characterize different AHSS grades: iCut (RFSR-CT-2015-0018), Tough-Sheet (RFSR-CT-2014-00015), OptiQPAP (RFCS-02-2015-709755) CrashTough (RFCS 800693) and MiPRE (RFCS 899268). The EWF may be considered a measure of the crack propagation.
- **Tearing Test:** This test method provides a measure of both notch toughness and resistance to crack propagation with the primary use as a screening or merit rank test. The significance of the tear test is similar to that of the notch-tensile test, and its primary usefulness is as an indicator of toughness or as a ranking test. The unit propagation energy (UPE) is the primary result of the tear test. This value provides a measure of the combination of strength and ductility that permits a material to resist crack growth under either elastic or plastic stresses. The UPE value has significance as a relative index of fracture toughness.
- **Nanoindentation Test:** Nanohardness measurements will be performed to evaluate the micromechanical properties of individual microstructural constituents and the hardness distribution along the analyzed area. Nanohardness maps are useful to detect small hardness variations and can be helpful to interpret the distribution of microstructural constituents and its influence on deformation and fracture behavior. The methodology is described by ISO 14577-1:2015 standard.

Formability has also been identified as a subject to study in section 2.6. So far, the literature clearly indicates a potential risk of loss of ductility during hot stamping related to the presence of the residual elements. Thereby, COOPHS project aims at providing the needed experimental data to assess this potential risk in ultrahigh press hardened steels with increasing content of embrittling elements. The main techniques that will be applied for this are:

- **Hot tensile testing:** is used to determine the hot rheology of the austenitic phase at high temperatures (between 600°C and 800°C). Strain hardening curves are measured at different strain rates to establish the sensitivity of the hot phase to sustain the forming process. In case of too high local necking during forming process, this can result in the failure of the part. The ductility draught induced by the presence of residual elements is typically in this range of temperature.
- **Formability study tooling:** High temperature forming trials will be performed in the Gestamp laboratory (Sweden) semi-industrial press hardening line using a tooling dedicated to formability studies. The tooling is internally designed with the purpose to evaluate different aspects in forming such as stretching at corners, radius and forming height. The stamped geometry is non-symmetrical covering various levels of complexity. The tooling is also used to verify that the material model and tensile test data correlates with physical outcome.

Finally, the study of hydrogen embrittlement has been found to be relevant in section 2.7.

First, for charging and measuring hydrogen, coophs will be using the following techniques:

- **Room temperature cathodic charging and high temperature furnace charging,** in which hydrogen diffuses into the steel after dissociation of the water molecule adsorbed at the surface of the steel from humidity in the air atmosphere. Absorbed

hydrogen is measured by Thermal Desorption Spectroscopy, based on hot gas extraction technique. Sample is put in a dedicated measuring chamber and heated up to defined temperature in order to enhance and assure hydrogen effusion out of the metal under a flow of carrier gas, typically nitrogen. Gas flow is then detected and analyzed by a mass spectrometer. Device calibration is carried out by certified gas mixtures.

- Electrochemical permeation tests: Hydrogen diffusivity in steel can be assessed by means of electrochemical hydrogen permeation test. This technique can return information on the hydrogen diffusion coefficient and consequently the presence of hydrogen traps in steel. Reference standard is the EN ISO 17081:2014.

For the study of hydrogen embrittlement testing involves applying an external stress on the hydrogen charged samples and for press hardening application the most relevant modes of deformation are plane strain by bending and uniaxial tensile by tensile tests. The techniques to be applied are the following:

- Delayed Fracture Resistance - Four Point Bending Test: Four point bending tests are carried out on hydrogen pre-charged specimens to characterize the delayed fracture behavior. Samples is loaded at defined level and periodically checked to identify any crack initiation, if no crack starts within 96h, samples is safe. Hydrogen content and failure load level are correlated to create a fracture map and a domain for safe application is determined.
- Slow Strain Rate tests: Slow Strain rate tests are performed on samples pre-charged with hydrogen, reference standard is the ASTM G129-21. It consists in a tensile test characterized by very low strain rate, this allows hydrogen to diffuse in the metal lattice and eventually accumulate at critical areas to give rise to embrittlement phenomenon. Mechanical parameters as tensile strength and elongation at break can be determined and correlated to diffusible hydrogen content to extrapolate a threshold value for the steel under investigation. Experimental data are thus interpolated with dedicated regression curve and the critical value is assumed as the hydrogen concentration correspondent to a 30% reduction of the considered mechanical property (STP 962) as shown in Figure 12.

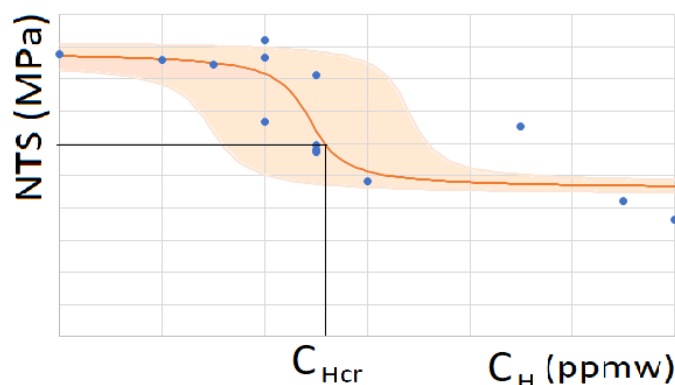


Figure 12: NTS vs CH experimental data, solid line shows the regression curve and shaded areas the confidence interval. Critical hydrogen content ( $CH_{cr}$ ) is determined in correspondence to a reduction of 30% of tensile strength

Finally, the issue of stress corrosion cracking resistance involves an alternative source of hydrogen; instead of hydrogen already present in the matrix introduced furnace charging the hydrogen entry in a consequence of localised corrosion phenomena. In order to study this for press hardening applications an external stress is applied either in bending or tension under corrosive conditions. The main testing methodology adopted for this study is:



- Four Point Bending Test under Corrosive Conditions: Four point bending tests are here performed at constant load given by a fixed deflection level and subjected to a corrosive environment. Different alternatives exist for the choice of corrosion environment: i) immersion in 5%NaCl water pH7, ii) Salt Spray test (5%NaCl), iii) Cyclic corrosion tests alternating wet and dry/hot and cold phases and iv) immersion in HCl acid pH1. From these options, those considering immersion and 5%NaCl water pH7 and cyclic corrosion tests are considered the most representative of actual application and will be applied in this project.

#### 3.2.4 Phase 4: Determination of key relationships between surface and grain boundary segregation of residual element and phase transformation, ductility, toughness and embrittlement behaviors

In this phase the challenge is to first derive quantitative parameters representing the segregation state of the different grain boundaries and surfaces present in the press hardened microstructures: martensite and bainite. This has been reported before as atomic percentage at grain boundaries for the elements under analysis by atom probe tomography and NanoSIMS using line scanning. Similarly these results can be expressed in atoms cm<sup>-2</sup> and derived terms of percentage of coverage of a monolayer. In this work all the techniques applied in Phase 2 will provide inputs for a representative quantification of the segregation states. This quantification exercise will allow, in a first deep analysis; a proposed link with grain boundary misorientation  $\omega$  considered the most influential crystallographic parameter along with grain boundary plane and rotation axis. This first phase of analysis will provide insight into the nature of key grain boundaries in these phases between high misorientation, low misorientation and twin boundaries regarding segregation behavior.

Once the segregated state of boundaries and surface has been quantified for the key elements of interest Cu, Sn, Sb, Ni, Mo, P, S; the analysis will be focused on the test results and fractographies obtained for the study of toughness, ductility, high temperature formability and hydrogen embrittlement resistance. From the results and observations, the levels of fracture stress and the boundaries associated to fracture will be derived. This phase aims at establishing relationships between the segregation state of boundaries and the cohesive strength of those boundaries leading to macroscopic results of performance tests. In the case of hardenability and phase transformation studies, the presence of B segregated in grain boundaries of different nature will be quantified and linked to the critical quenching rate for martensitic or bainitic transformation.

This phase aims at applying a scientific approach to the analysis of results based on observations, hypothesis and synthesis of results. Mechanisms are proposed and discussed in the light of prior research and present results.

#### 3.2.5 Phase 5: Identification of the optimum compromise of CO<sub>2</sub> emission levels and product and application performance of ultrahigh strength press hardened steels

This phase is focused on the analysis of the product performance results in terms of in-use properties, among many others: tensile strength, ductility and bendability values, high temperature formability limits, impact toughness transition temperatures and Upper Shelf Energy, hydrogen embrittlement index and Critical hydrogen content for a given applied stress below which the applications are safe. The large database collected in this project will be analyzed with a datamining approach deriving areas of safe application of the press hardened products under study comprising different levels of residual elements and therefore different levels of CO<sub>2</sub> emission involved in their production. With properties characterizing simultaneously performance in mechanical properties, ductility, toughness, crash resistance and hydrogen induced resistance a multi-axis approach is required for which datamining



methodologies will be applied from a simple correlation approach using tools such as Orange Software to Python modeling of interactions in the most complex cases. The output of this analysis will be expressed as the overlapping areas of safe behavior and optimum performance of the materials under study. These overlapping areas will be associated to the levels of CO<sub>2</sub> emissions calculated in Phase 2 and will provide a clear indication of the areas of applications of press hardened products with different CO<sub>2</sub> imprints. The assessment of these safe overlapping areas will provide at the same time the optimum compromise between product performance and CO<sub>2</sub> emission levels and the range of application of all products in the wide range of production routes and CO<sub>2</sub> emission levels.

In this phase it is also aimed a discussion on the impact of the low CO<sub>2</sub> routes on the final application of ultrahigh strength press hardening steel considering two key cases: i) B Pillar and ii) Battery Pack shield in electric vehicles. These cases have been selected as the performance requirements differ notably in terms of three aspects: high temperature formability, crash resistance and corrosion exposure and therefore hydrogen induced stress corrosion resistance. While B-Pillar applications have strong constraints in terms of formability and crash resistance, a critical aspect of battery pack shield is the high severity of corrosion exposure. This discussion will be supported by simulations on the behaviors of these parts in real life.

## 4. Objectives and Outcomes

---

Based on the state of the art described in section 2, on the identification of the problem to be solved (section 3.1) and the remaining research challenges, an approximation based on phases has been proposed. The aim of these phases is to tackle specific project objectives, defined with KPIs. The objectives defined in COOPHS are the following:

- **Determine the impact of low CO<sub>2</sub> steel processing routes on the compositional changes of ultrahigh strength steel grades for press hardening**, notably regarding the content of residual elements associated to EAF steel production routes: Cu, Sn, Ni, Sb, P, N, S and the consequences in terms of microstructures considering mainly grain boundary and surface segregation phenomena.
  - KPI: Local concentrations of residual elements (atoms.cm<sup>-2</sup>) as a function of boundary type in hot stamped microstructures and nominal composition.
- **Determine the impact of these local residual elements segregations on key properties of press hardened steels product** from standard hot stamping processes (autotempered martensite) and non-standard ones (tempered martensite and martensite-bainite designs): Hardenability and temper embrittlement resistance, Toughness and Ductility, Hot Formability and Hydrogen embrittlement resistance. The aim is to determine the key segregated boundaries and the segregation rates that affect, dominate or control the material behavior.
  - KPI: Upper limits of residual elements as a function of grade strength for key in use properties.
- **Develop a tool to optimize the compromise between CO<sub>2</sub> emissions and product and application requirements to facilitate the progression of low CO<sub>2</sub> steels in the PHS automotive market.** The aim is to provide a map of overlapping areas for safe application of these products in terms of product and application requirements for a wide scope of CO<sub>2</sub> emissions.
  - KPI: Safe application areas for low CO<sub>2</sub> steels representing a minimum of 50% of current press hardened steels applications in Europe.
- **Establish a comparative positioning of EAF based low CO<sub>2</sub> ultrahigh strength press hardening steel solutions related to the current BOF based standard** in terms of hot stamping process windows, key product properties and application guidelines.



- KPI: Distinctive product and process features.
- Propose optimised low emission processing routes of high-performance steels that strengthen the European steel market respect to global material producers, keeping the employment and growing of the industry.

By accomplishing these objectives, project COOPHS will provide valuable scientific and technological progress on the following key areas:

- Qualitative and quantitative characterization of the simultaneous segregation of residual elements Cu, Sn, Sb, Ni, Mo and that of P and S at grain boundaries of different nature (misorientation angle) in ultrahigh martensitic steels microstructures obtained by short austenitization treatments followed by die quenching. This will combine segregation in  $\gamma$ -Fe phase and potential changes introduced by phase transformation and autotempering in  $\gamma$ -Fe.
- Qualitative and quantitative characterization of the simultaneous segregation of residual elements Cu, Sn, Sb, Ni, Mo and that of P and S at the surface of the steel at the hot stamped state and their diffusion and enrichment across the alloyed coating revealing compositional and structural changes.
- Interactions between segregation of B and residual elements (Cu, Sn, Sb, Ni, Mo) in austenite under conditions of hot stamping combining the effect of cooling rates and deformation and determination of the impact on steel hardenability and the progress of phase transformation during quenching.
- Qualitative and quantitative characterization of the role of the combined segregation of residual elements (Cu, Sn, Sb, Ni, Mo) and P, S, B and H in austenite on the hot formability limits ultrahigh strength steels in the range of temperatures, strain and strain rates associated to hot stamping.
- Impact of combined residual elements segregation (Cu+Sn+Sb) along with those known of P and S on the cohesive strength of grain boundaries in ultrahigh martensitic steels microstructures and their role on Hydrogen enhanced decohesion (HEDE) mechanisms dominating the hydrogen induced embrittlement and triggering intergranular fracture under applied stresses.
- Impact of combined residual elements segregation (Cu+Sn+Sb) along with those known of P and S on the cohesive strength of grain boundaries in ultrahigh martensitic steels microstructures and their role on Temper Embrittlement mechanisms under conditions of autotempering and tempering treatments applied in press hardening steel notably by localized softening treatment (laser).
- Comparative characterization of in-use properties of ultrahigh press hardened steels from EAF and BOF processing routes in the range of strength 1500-1800MPa and impact of the scope of applications of low CO<sub>2</sub> Press Hardening Steels

## 5. References

---

[ArcelorMittal 2021] ArcelorMittal [Online] July 7, 2021 [https://corporate-media.arcelormittal.com/media/y24ivh2y/arcelormittal-net-zero-steel-presentation\\_12-07-21-final-for-website.pdf](https://corporate-media.arcelormittal.com/media/y24ivh2y/arcelormittal-net-zero-steel-presentation_12-07-21-final-for-website.pdf)

[ArcelorMittal2] Steels for hot stamping - Usibor® and Ductibor® – [https://automotive.arcelormittal.com/products/flat/PHS/usibor\\_ductibor](https://automotive.arcelormittal.com/products/flat/PHS/usibor_ductibor)

[ArcelorMittal3] Steels coated with Alusi®, an aluminium-silicon alloy – <https://automotive.arcelormittal.com/products/flat/coatings/alusi>



- [Asahi 2002] H. Asahi; 'Effects of Mo addition and austenitizing temperature on hardenability of low alloy B-added steels', *ISIJ Int.*42(2002)1150–1155
- [ASM 1996] J.R. Davis. Thermal Induced Embrittlement of Steels, ASM Specialty Handbook: Carbon and Alloy Steel. ASM International (1996)
- [BDSV 1995] Steel Scrap Specification Bundesvereinigung Deutscher Stahlrecycling- und Entsorgungsunternehmen e.V. – June 1995
- [Beachem 1972] Beachem CD; 'A new model for hydrogen-assisted cracking (hydrogen "embrittlement")'. *Metall Trans* 1972;3:441-455.
- [Biereis 2017] M.Biereis, L.Wu, L.Santos, M.Masoumi, F.da Rocha Filho; 'Role of lattice strain and texture in hydrogen embrittlement of 18Ni (300) maraging steel'. *Int J Hydrogen Energy* 2017; 42: 14786.
- [Brosse 2022] G Brosse, « EAF premelter Bremen; Metallurgical aspects » Internal communication 28/01/22
- [Calvo-Muñoz 2006] Calvo Muñoz, Jessica. Efecto de los elementos residuales e impurezas en la ductilidad y mecanismos de fragilización en caliente de un acero de construcción 0.23C-0.9Mn-0.13Si. PhD thesis, Universitat Politècnica de Catalunya (2006)
- [Chen 2020] 49. Y.S. Chen, H.Lu, J.Liang, A.Rosenthal, H.Liu, G.Sneddon, I.McCarroll, Z.Zhao, W.Li, A.Guo, J. Cairney; 'Observation of hydrogen trapping at dislocations, grain boundaries, and precipitates'. *Science* 2020;367:171e5.
- [Christien 2011] F. Christien, R. Le Gall; Ultra-fast grain boundary diffusion and its contribution to surface segregation on a martensitic steel. *Experiments and modeling, Surface Science* 605 (2011) 1711–1718
- [Daehn 2027] Katrin E. Daehn, AndréCabrera Serrenho, and Julian M. Allwood. How Will Copper Contamination Constrain Future Global Steel Recycling? *Environmental Science % Technology* 51 (2017), <https://doi.org/10.1021/acs.est.7b00997>
- [de Caro 2023] De Caro D, Tedesco MM, Pujante J, Bongiovanni A, Sbrega G, Baricco M, Rizzi P. Effect of Recycling on the Mechanical Properties of 6000 Series Aluminum-Alloy Sheet. *Materials (Basel)*. 2023 Oct 20;16(20):6778. doi: 10.3390/ma16206778. PMID: 37895758; PMCID: PMC10608306.
- [Dong 2022] F.Dong, J.Venezuela, H.Li, Z.Shi, Q.Zhou, L.Chen, J.Chen, L.Du, A.Atrens; 'The influence of phosphorus on the temper embrittlement and hydrogen embrittlement of some dual-phase steels', *Materials Science & Engineering A* 854 (2022) <https://doi.org/10.1016/j.msea.2022.143379>
- [Dworak 2021] Sabine Dworak, Johann Fellner, Steel scrap generation in the EU-28 since 1946 – Sources and composition, *Resources, Conservation and Recycling*, Volume 173, 2021, ISSN 0921-3449, <https://doi.org/10.1016/j.resconrec.2021.105692>.
- [Erbehart 1987] M.E.Eberhart, D.Vvedensky; 'Localized grain-boundary electronic states and intergranular fracture'. *Phys Rev Lett* 1987; 58: 61-65.
- [Eurofer 2020] EUROFER; A Green Deal on Steel. [Online] April 1, 2020 <https://www.eurofer.eu/issues/climate-and-energy/a-green-deal-on-steel/>
- [Georgiadis 2017] G. Georgiadis, A. E. Tekkaya, P. Veigert, S. Horneber, P. Aliage Kuhnle, 'Formability analysis of thin press hardening steel sheets under isothermal and non-isothermal condition', *Int J Mater* (2017), 10:405-19
- [Guo 2019] X.H. Guo, Y.D. Zhang, S.B. Jin, R. Hu, Z.W. Liu, R.Q. Zhang, G. Sha; 'Segregation and precipitation at grain boundaries of weathering steels without/with Sb addition' *Materials Chemistry and Physics* 236 (2019) 121783



- [Guttman 2001] M. Guttman. Interfacial segregation and temper embrittlement. Encyclopedia of Materials: Science and Technology. Elsevier, Oxford (2001)
- [Gyllenram 2015] R.Gyllenram, W.Wei, P.Jonsson; 'Raw material assessment for electric arc furnace steelmaking' May 2015 Conference: The 6th International Congress on the Science and Technology of Steelmaking (ICS2015): Beijing, China
- [Han 2008] F.Han, B.Hwang, D.W.Suh, Z.Wang, D.L.Lee, S.J.Kim; 'Effect of molybdenum and chromium on hardenability of low-carbon boron-added steels', *Met.Ma-ter.* 14(2008)667–672.
- [Hara 2004] T.Hara, H.Asahi, R.Uemori, H.Tamehiro; 'Role of combined addition of niobium and boron and of molybdenum and boron on hardenability in low carbon steels', *ISIJInt.* 44(2004)1431–1440.
- [He 1989] X.L. He, Y.Y.Chu, J.J.Jonas; 'Grain boundary segregation of boron during continuous cooling', *ActaMetall.* 37(1989)147–161.
- [He 2017] X.He, Sh.Wu, L.Shia, D.Wang, Y.Dou, W.Yang; 'Grain Boundary Segregation of Substitutional Solutes/Impurities and Grain Boundary Decohesion in BCC Fe Energy Procedia 127 (2017) 377–386
- [HSSinsights] PHS Automotive Applications and Usage; 'World Steel Auto - PHS Automotive Applications and Usage - AHSS Guidelines (ahssinsights.org)
- [ISPAT] Dephosphorization of Steels; Dephosphorization of Steels – IspatGuru Dephosphorization of Steels – IspatGuru <https://www.ispatguru.com/dephosphorization-of-steels/>
- [Kazuma 2022] I.Kazuma, S.Hideaki; 'First-principles analysis of the grain boundary segregation of transition metal alloying elements in  $\gamma$ Fe' *Computational Materials Science* 210 (2022) 11 1050
- [Komazazki 2003] S. Komazazki, S. Watanabe, T. Misawa, 'Influence of Phosphorus and Boron on Hydrogen Embrittlement Susceptibility of High Strength Low Alloy Steel', *ISIJ Int.* 43(2003) 1851–1857.
- [Kulkov 2018] S.Kulkov, A.Bakulin, S.Kulkova; 'Effect of boron on the hydrogen-induced grain boundary embrittlement in  $\alpha$ -Fe' *International Journal of hydrogen energy* 43 (2018) 1909 - 1925
- [Lee 1984] D.Y.Lee, E.Barrera, J.Stark, H.Marcus; 'The influence of alloying elements on impurity induced grain boundary embrittlement'. *Metall Trans A* 1984; 15:1415-1445.
- [Lee 2015] B Lee; 'Effect of Hot metal on decarburization in the EAF and dissolved Sulfur, Phosphorous and nitrogen content in steel', *ISIJ*, Vol 55, 2015, N 3
- [Lin 2015] Y.J.Lin, D.Pongen, P.Choi, D.Raabe; 'Atomic scale investigation of non-equilibrium segregation of boron in a quenched Mo-free martensitic steel' *Ultramicroscopy* 159(2015)240–247
- [Mai 2022] H.Mai, X.Cui, D.Scheiber, L.Romaner, S.Ringer; 'The segregation of transition metals to iron grain boundaries and their effects on cohesion' *Acta Materialia* 231 (2022) 117902
- [Martin 2019] M.L.Martin, M.Dadfarnia, A.Nagao, S.Wang, P.Sofronis; 'Enumeration of the hydrogen-enhanced localized plasticity mechanism for hydrogen embrittlement in structural materials'. *Acta Mater* 2019;165:734e50
- [Materkowski 1979] J.P. Materkowski, G. Krauss, *Metallurgical Transactions A*, 10 (1979) 1643-1651



- [Matsuoka 1997] H. Matsuoka, K. Osawa, M. Ono, M. Ohmura, 'Influence of Cu and Sn on hot ductility of steels with various C content', ISIJ International, Vol. 37 (1997), pp. 255-262.
- [McKinsley 2020] World Economic Forum and McKinsey; Forging Ahead: A materials roadmap for the zero-carbon car. Geneva / Switzerland; World Economic Forum, 2020
- [McLean 1957] D. McLean; 'Grain Boundaries in Metals', Oxford University Press, London, 1957.
- [Mincu 2013] V.Mincu, N.Constantin; 'Refining steels produced in electric arc furnaces', U.P.B. Sci. Bull., Series B, Vol. 75, Iss. 2, 2013
- [Mun 2012] D.J. Mun, E.J.Shin, K.C.Cho, J.S.Lee, Y.M.Koo; 'Cooling rate dependence of boron distribution in low carbon steel', Metall.Mater.Trans.A43(2012) 1639–1648.
- [Nakajima 2011] Kenichi Nakajima, Osamu Takeda, Takahiro Miki, Kazuyo Matsubae, Tetsuya Nagasaka. Thermodynamic analysis for the controllability of elements in the recycling process of metals. Environmental science & technology 45 (2011).
- [Noro 1997] Katsuhiko Noro, Mitsugu Takeuchi, Yoshimasa Mizukami, Necessity of Scrap Reclamation Technologies and Present Conditions of Technical Development, ISIJ International, 1997, Volume 37, Issue 3, Pages 198-206
- [Peng 2015] H-B Peng, W-Q Chen, D. Guo, 'Effect of Tin, Copper and Boron on the hot ductility of 20CrMnTi steel between 650°C and 1100 °C', High Temp. Mater. Proc.. 2015; 34(1):19-26.
- [Petrovic 2006] D.Petrovic, M.Jenko, M.Jeram, F.Marinsek and V.Presern; 'The surface segregation of impurity elements in non-oriented electrical steels' Strojarstvo 48 (1-2) 45-49 (2006)
- [Poole 2011] W.J.Poole, J.D.Embury, D.J.Lloyd Work hardening in aluminium alloys. Woodhead Publishing Series in Metals and Surface Engineering (2011)
- [Rice 1989] J.R. Rice and J-S.Wang; 'Embrittlement of Interfaces by Solute Segregation', Materials Science and Engineering, A1 07 (1989) 23-40 23
- [Rod 2006] O. Rod, C. Becker, M. Nylén, KIMAB. Opportunities and dangers of using residual elements in steels: a literature survey. Jernkontorets Forskning, JK88042 (2006)
- [Savov 2003] Luben Savov, Elena Volkova, Dieter Janke, Copper and Tin in Steel Scrap Recycling. RMZ Materials and Geoenvironment 50 (2003)
- [Scheiber 2020] D. Scheiber, K. Prabitz, L. Romaner, W. Ecker; 'The influence of alloying on Zn liquid metal embrittlement in steels', Acta Mater 195 (2020) 750–760.
- [Tahir 2014] A.Tahir, R. Janisch, A.Hartmaier; 'Hydrogen embrittlement of a carbon segregated S5(310)[001] symmetrical tilt grain boundary in  $\alpha$ -Fe'. Mater Sci Eng A 2014; 612: 462-469.
- [Ueno 1988] M.Ueno, K.Itoh; 'The optimum condition to obtain the maximum hardenability effect of boron', Tetsu-to-Hagané 74 (1988) 910–917.
- [Vass 2021] T. Vass, P. Levi, A. Gouy, H. Mandova; Iron and Steel, IEA [Online] International Energy Agency; November 2021 <https://www.iea.org/reports/iron-and-steel>
- [Vergani 2014] L.Vergani, C.Colombo, G.Gobbi, F.Bolzoni, G.Fumagalli; 'Hydrogen effect on fatigue behavior of a quenched & tempered steel'. Process Eng 2014;74:468-471.
- [Weng 2001] W.T.Geng, A.J.Freeman, G.B.Olson; 'Influence of alloying additions on grain boundary cohesion of transition metals: first-principles determination and its phenomenological extension'. Phys Rev B 2001;63.





[Yamaguchi 2007] M.Yamaguchi, Y.Nishiyama, H.Kaburaki; 'Decohesion of iron grain boundaries by sulfur or phosphorous segregation: first principles calculations'. Phys Rev B 2007;76.

[Yamaguchi 2011] M.Yamaguchi, K.Ebihara, M.Itakura, T.Kadoyoshi, T.Suzudo, H.Kaburaki; 'First-principles study on the grain boundary embrittlement of metals by solute segregation: Part II. Metal (Fe, Al, Cu)-hydrogen (H) systems'. Metall Mater Trans A 2011; 42: 330-339.

[Zhang 2022] Y. D. Zhang, S. B. Jin, C. L. Jiang, J. Yang, G. Sha, 'Formation of high temperature inner oxide scale on low alloy steels: segregation, partitioning and transformation reactions', Corrosion science 195 (2022), 109980.

[Ziliu 2021] Ziliu Xiong, Zhanguo Lin, Jianjun Qi, Li Sun, Guangxin Wu, Shuang Kuang, and Guoping Zhou; 'Research on high-temperature oxidation resistance, hot forming ability, and microstructure of Al-Si-Cu coating for 22MnB5 steel', High Temperature Materials and Processes 2021; 40: 397-409